

Comparison of Lower Arm Weight and Passive Elbow Joint Impedance Compensation Strategies in Non-Disabled Participants

Filius, Suzanne; Janssen, Mariska; Kooij, Herman van der; Harlaar, Jaap

DOI

[10.1109/ICORR58425.2023.10304707](https://doi.org/10.1109/ICORR58425.2023.10304707)

Publication date

2023

Document Version

Final published version

Published in

Proceedings of the 2023 International Conference on Rehabilitation Robotics (ICORR)

Citation (APA)

Filius, S., Janssen, M., Kooij, H. V. D., & Harlaar, J. (2023). Comparison of Lower Arm Weight and Passive Elbow Joint Impedance Compensation Strategies in Non-Disabled Participants. In *Proceedings of the 2023 International Conference on Rehabilitation Robotics (ICORR)* IEEE.
<https://doi.org/10.1109/ICORR58425.2023.10304707>

Important note

To cite this publication, please use the final published version (if applicable).
Please check the document version above.

Copyright

Other than for strictly personal use, it is not permitted to download, forward or distribute the text or part of it, without the consent of the author(s) and/or copyright holder(s), unless the work is under an open content license such as Creative Commons.

Takedown policy

Please contact us and provide details if you believe this document breaches copyrights.
We will remove access to the work immediately and investigate your claim.

Green Open Access added to TU Delft Institutional Repository

'You share, we take care!' - Taverne project

<https://www.openaccess.nl/en/you-share-we-take-care>

Otherwise as indicated in the copyright section: the publisher is the copyright holder of this work and the author uses the Dutch legislation to make this work public.

Comparison of Lower Arm Weight and Passive Elbow Joint Impedance Compensation Strategies in Non-Disabled Participants*

Suzanne Filius¹, Mariska Janssen², Herman van der Kooij^{1,3}, Jaap Harlaar^{1,4}

Abstract—People with severe muscle weakness in the upper extremity are in need of an arm support to enhance arm function and improve their quality of life. In addition to weight support, compensation of passive joint impedance (pJimp) seems necessary. Existing devices do not compensate for pJimp yet, and the best way to compensate for it is still unknown. The aim of this study is to 1) identify pJimp of the elbow, and 2) compare four different compensation strategies of weight and combined weight and pJimp in an active elbow support system. The passive elbow joint moments, including gravitational and pJimp contributions, were measured in 12 non-disabled participants. The four compensation strategies (*scaled-model*, *measured*, *hybrid*, and *fitted-model*) were compared using a position-tracking task in the near vertical plane. All four strategies showed a significant reduction (20-47%) in the anti-gravity elbow flexor activity measured by surface electromyography. The pJimp turned out to contribute to a large extent to the passive elbow joint moments (range took up 60%) in non-disabled participants. This underlines the relevance of compensating for pJimp in arm support systems. The parameters of the scaled-model and hybrid strategy seem to overestimate the gravitational component. Therefore, the measured and fitted-model strategies are expected to be most promising to test in people with severe muscle weakness combined with elevated pJimp.

I. INTRODUCTION

Pathologies such as Muscular Dystrophies (MD), Stroke, Spinal Muscular Atrophy (SMA) and Amyotrophic Lateral Sclerosis can result in severe arm muscle weakness and consequential functional loss. These patients are in need of arm support(s) to regain arm function and improve their independence, social participation and quality of life. It has been shown that people with arm disabilities benefit from weight compensation by arm supports to assist activities of daily living (ADL) [1], [2].

Besides the support of arm weight, compensation of passive joint impedance (pJimp) seems necessary in pathologies (e.g., MD, SMA) with severe muscle weakness in combination with elevated pJimp [3], [4]. The pJimp is

*This work is part of the research program Wearable Robotics with project number P16-05, which is funded by the Dutch Research Council (NWO) The Netherlands, Duchenne Parent Project, Spieren voor Spieren, Festo, Yumen Bionics, Baat Medical and the FSHD society.

¹ S.Filius, H.van der Kooij, and J. Harlaar are with Mechanical, Marine and Materials Engineering, Technical University of Delft, Delft, 2628CD, The Netherlands. s.j.filius@tudelft.nl

² M. Janssen is with Department of Rehabilitation, Donders Institute for Brain, Cognition and Behaviour, Radboud University Medical Center, Nijmegen, 6525 GD, The Netherlands.

³ H. van der Kooij is also with Department of Biomechanical Engineering, University of Twente, Enschede, 7522 NB, The Netherlands.

⁴ J. Harlaar is also with Department of Orthopedics and Sports Medicine, Erasmus MC University Medical Center, Rotterdam, 3015 GD, The Netherlands.

expressed as the passive resistance in response to a joint movement [5], [6], so not the active resistance that result from (involuntary) muscle activation (e.g., spasticity). In some pathologies like Duchenne MD (DMD) the pJimp can be 5 times the residual muscle strength [4]. Previous studies have highlighted the clinical relevance of pJimp compensation in people with DMD [7], [8], [3] and shown that with only weight compensation the functional gain was limited [4]. In weakened individuals with elevated pJimp, the ratio between the voluntary and passive forces (e.g., gravitational and pJimp) is very small and difficult to distinguish from each other [3]. Moreover, pJimp can change as the disease progresses [9], [10], but it can also vary throughout the day, through room temperature changes [11] or by doing stretching exercises [12]. This makes it difficult to model and compensate for pJimp [4].

Ragonesi et al. [3] measured the passive arm dynamics in non-disabled and adolescents with neuromuscular disabilities (i.e., MD, Arthrogyrosis and SMA) for arm support purposes. They measured the passive elbow and shoulder joint moments in the vertical (e.g., sagittal) plane using static measurements over ca. 72 postures. Lobo-Prat et al. [8] measured the passive elbow joint moments in MD patients dynamically at slow velocity (2.9°/s) over the elbow range of motion (ROM) and compensated for it in an active elbow support system. Unfortunately, both methods are time consuming and become complex when translating it to multiple degrees of freedom (DOF). Moreover, since the pJimp varies over time, these calibration measurements need to be repeated regularly. Therefore, new strategies to compensate for a combination of weight and pJimp are required that are less time consuming and complex. Modelling the pJimp would reduce the need for (re)calibration processes, since it allows for parameter tuning. Another option is to add a single plane measurement of the pJimp to a scaled gravitational model. Those two approaches will be explored and compared to the existing (i.e. scaled gravitational model [13] and measured passive joint moments [8]).

This study aims to 1) identify passive elbow joint impedance, and 2) compare four different compensation strategies of weight and combined weight and pJimp in an active elbow support system in non-disabled participants.

II. METHODS

A. Participants

For this study, 12 non-disabled male individuals between 18 and 35 years old were recruited with no history of arm injuries, joint dislocations, or movement difficulties nor active

implants (e.g., pacemaker). Ethical approval was obtained from the Human Research Ethics Committee (HREC) from Technical University of Delft (ID2284). All participants gave written informed consent before participation.

B. Equipment

Fig. 1 shows the two configurations used in the active elbow system. The actuator is aligned with the elbow joint (φ), and the frame is adjustable in shoulder abduction angle (θ) and height. The horizontal configuration ($\theta = 90^\circ$) was used to measure pJmp and the combined passive joint moments were measured in the near vertical configuration ($\theta = 15^\circ$) to avoid collision with the body. Distal of the actuator, a sleeve interface holds the forearm of the participant in a neutral orientation (thumb upward).

The elbow joint angle was measured by absolute encoders (ICHaus, Germany), with a resolution of 19 bits, attached to a custom sensor slave running at 1 kHz. A 6 DOF force/torque (F/T) sensor (SI-40-mini F/T, Schunk, ATI Industrial Automation, USA) was placed on the forearm at the sleeve interface, to measure the interaction forces, converted to express the elbow joint torque. The analog signal of the F/T sensor was digitized to 12 bits at 1 kHz. The encoders and F/T sensor were connected over EtherCAT to a computer and interfaced using TwinCAT 3, Beckhoff Automation, Verl, Germany. For each experiment the F/T sensor was calibrated. Surface electromyography (sEMG) signals were recorded with Delsys® Trigno Avanti™ Sensors that communicate with Bluetooth BLE 4.2. The analog signal was sampled at 1.1 kHz with a 16 bits analog-to-digital converter internally. The Delsys® software EMGWorks was used for real-time visualization of the sEMG signals and storing the signals. The skin preparation and sensor placement on the short head of the m. biceps brachii and the lateral head of the m. triceps brachii were in accordance with the SENIAM guidelines [14]. The encoders, F/T sensor and sEMG signals were synchronized using a 5V trigger signal.

C. Outcome measures

The primary outcome measure was the compensation efficacy measured in the position-tracking task (day 2). This was defined by the root mean square (RMS) of the sEMG signals of biceps and triceps muscles, where a lower RMS sEMG indicates higher compensation efficacy. Secondary outcome measures were the RMS of the position-tracking error (since this affects the sEMG signals); the task workload using the NASA-Task Load index (NASA-TLX); a subjective 5-point Likert Scale (1 dislike, 5 like); and the personal preference for a specific compensation strategy. The NASA-TLX evaluates the workload of a task on 6 rating scales (e.g., mental demand, physical demand, temporal demand, performance, effort, and frustration).

D. Study design

The study consisted of 3 sessions divided over 2 days. First the biometric data (i.e., body mass, body length, arm segment lengths, and hand plus forearm segment volumes)

were collected to calculate weight and center of mass (COM) of the forearm and hand using anthropometric tables [15]. For the weight calculation, the segment volumes were measured using the water displacement method [16] and were multiplied with an averaged density value from cadaver studies [17], [18], [19].

Next, the actuator moved the arm of the participants held in the horizontal configuration through 80% of the range of elbow motion over 8 cycles while the participant was asked to fully relax the arm, at $2.9^\circ/s$ [8] and at $5.7^\circ/s$. Next, the elbow was moved in the near vertical plane at $5.7^\circ/s$.

On the second day, first 2 repetitions of the maximum voluntary contraction (MVC) for 3 seconds of the biceps and triceps muscles were collected. In the position-tracking task, the participants were asked to actively follow a sinusoidal (5 cycles of 20s each) target position signal at 75% of the total elbow ROM. The target position and the real-time elbow joint position were displayed on a screen in front of the participant and the participant was asked to follow the target line as close as possible, see Fig. 2. First a trial with the actuator turned off was performed to get familiar with the task. Then a baseline measurement was recorded, where the actuator was activated in zero-impedance mode [20]. After this, the four compensation strategies (*scaled-model*, *measured*, *hybrid*, and *fitted-model*) were compared in a randomized order and were provided with a gain of 80% since a gain of 100% is not always preferred [21], [22], [23]. Before each compensation strategy, a test trial was done to get familiar with the strategy. After each compensation strategy the (dis)like 5-point Likert scale and the NASA-TLX scores were collected. The NASA-TLX was collected using the official NASA Task Load Index (TLX) iOS app [24].

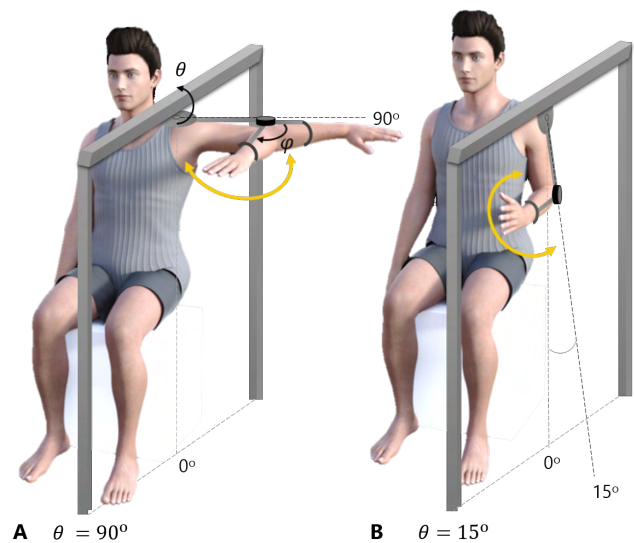


Fig. 1. Experimental set-up with A) the horizontal and B) the near vertical configuration. The actuator is represented by the black disc at the elbow joint. Note: model was retrieved from DAZ Productions (<https://www.daz3d.com/eula>).

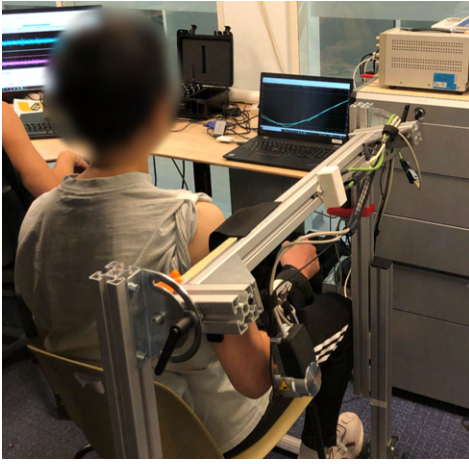


Fig. 2. Picture taken on experiment Day 2, with the real-time sEMG signals on the computer screen left and the position-tracking task on the computer screen on the right.

The four compensation strategies consisted of a *scaled-model* (i.e., compensates for weight only using a simplified kinetic model scaled to the individual biometric parameters), *measured* (i.e., compensates for the combined passive forces including weight and pJimp measured in the near vertical plane), *hybrid* (i.e., a combination of the scaled-model and the measured pJimp in the horizontal plane), and *fitted-model* (i.e., that combines the kinetic weight model with a linear pJimp model fitted to the measured passive forces in the near vertical plane). The formulas of the strategies are listed in Table I.

E. Data processing

Data selection: The first and last cycles and the cycles where the participant was not relaxed enough (where sEMG $> 3 \times SD$ of the 3 cycles with lowest average sEMG, with a spike allowance of 5% within the separate cycles) were excluded from analysis.

Passive joint moments: The measured passive joint moments depend on the movement direction [5]. For simplification, the joint moment at a specific angle was calculated by taking the average of the flexion and extension cycles. Moreover, to calculate the pJimp, the velocity conditions (2.9 and 5.7°/s) were combined and averaged.

sEMG processing: The sampled raw sEMG data was filtered with a 3th order high-pass Butterworth zero-phase

digital filter with a cut-off frequency of 20 Hz. Then, the envelope was taken by taking the absolute values and apply a 2nd order low-pass Butterworth zero-phase digital filter with a cutoff frequency of 1 Hz. The MVC was determined by taking the maximal value of the 2 attempts. The sEMG recorded during the compensation strategies was normalized to the MVC. The RMS values for the sEMG signals were calculated and compared among each condition. The specific samples where participants showed an overshoot of the target position outside of the measured 80% of ROM were excluded from analysis.

RMS tracking error: The RMS of the tracking error was calculated by taking the RMS of the error between the measured elbow joint angle and the target position signal.

All processing was done using custom programming in MATLAB®.

F. Statistics

Descriptive statistics were used to calculate the group mean (M), standard error of the mean (SEM) and standard deviation (SD). The distributions of the outcome measures were examined for normality of distribution to select either the parametric one-way repeated measure analysis of variance (ANOVA) or the non-parametric Friedman's ANOVA. Wilcoxon Signed Rank Tests were used in addition to the non-parametric Friedman's ANOVA for the pairwise comparison. The false discovery rate (FDR) was used to correct the level of significance for multiple pairwise comparisons [25], [26]. The effect size r was calculated by the z score divided by the number of observations squared [27]. Statistical analyses were performed using SPSS (IBM SPSS Statistics for Windows, Version 28.0.1.0 (Armonk, NY, USA: IBM Corp.))

III. RESULTS

Twelve non-disabled male individuals participated in the study, see Table II for the descriptive characteristics.

The Shapiro-Wilk test revealed that the RMS of the triceps muscle and tracking error deviated from normal. Therefore, non-parametric tests were selected for all outcome measures.

The average joint moment profiles of the four compensation strategies evolving from the measurements performed on Day 1 are displayed in Fig. 3. The measurement of the pJimp in the horizontal plane showed a negative profile up

TABLE I
OVERVIEW OF COMPENSATION STRATEGY JOINT TORQUES

Strategy	Formula	Measured at
Baseline	$\tau_{GJ} = 0$	none
Scaled	$\tau_{Gmod} = q \cdot m \cdot com \cdot g \cdot \sin(\varphi) \cdot \cos(\theta)$	none
Hybrid	$\tau_{GmodJmeas} = q \cdot (\tau_{Gmod} + \tau_{Jmeas})$	$\theta = 90^\circ$
Measured	$\tau_{GmeasJmeas} = q \cdot (\tau_{Gmeas} + \tau_{Jmeas})$	$\theta = 15^\circ$
Fitted	$\tau_{GJfit} = q \cdot (m \cdot com \cdot g \cdot \sin(\varphi) \cdot \cos(\theta) + a\varphi + b)$	$\theta = 15^\circ$

Abbreviations: τ = torque, G = gravity, J = passive joint impedance, *mod* = modelled, *meas* = measured, q = gain, m = mass, *com* = center of mass, g = gravitational acceleration, φ = elbow joint angle, and θ = shoulder abduction angle

TABLE II
PARTICIPANT CHARACTERISTICS

$n = 12$ (Unit)	M	SD	95%CI
Age (years)	29	3.6	[26.5-31.5]
Weight (kg)	76.1	13.1	[67.1-85.1]
Body length (cm)	179.7	9.9	[172.9-186.5]
com _{forearm+hand} (m)	16.2	1.3	[15.3-17.0]
mass _{forearm+hand} (kg)	1.7	0.4	[1.4-1.9]
Dominant hand (r/l)	11/1	-	-
Frequency of sport (1-5)	2.6	1.1	[1.8-3.3]
Intensity of sport (1-5)	3.2	1.0	[2.5-3.8]

Abbreviations: n = number of participants; M = mean; SD = standard deviation; CI = confidence interval; *com* = center of mass.

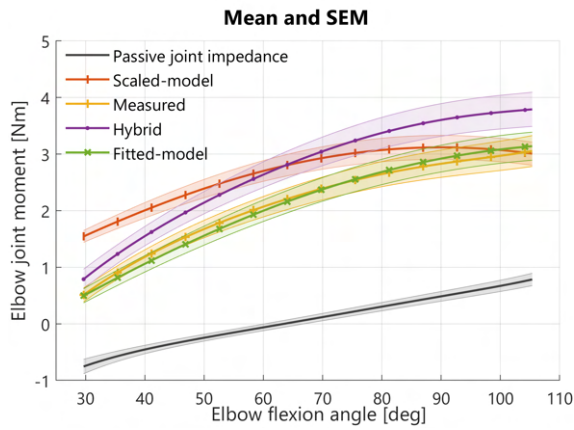


Fig. 3. Group mean and standard error of the mean (SEM) results of the torque-angle profiles of the four compensation strategies and the measured pJimp. Based on the data of day 1 (relaxation task).

to the equilibrium of the elbow joint (e.g., where it crosses zero) around 65° elbow flexion. Note that elbow flexion range presented in this graph is limited to the commonly shared ROM of the group, each individual ROM is larger. The measured pJimp was larger near the limits of the elbow joint, and varied between -2.2 and 2.1 Nm. The individual measured joint torques in the near vertical plane crossed the zero towards the elbow extension (at ca. $17\text{-}25^\circ$) in most cases and varied between -0.9 and 5.8 Nm. On average, the range of measured pJimp took up 60% ($\pm 14\%$) of the total range of the measured passive forces. The mean absolute difference between the flexion and extension cycles due to the aforementioned direction dependency in the muscles [5] was approximately < 0.5 Nm on average. The mean absolute difference in slope between the two velocities measured in pJimp was $2.7e^{-3} (\pm 2.6e^{-3})$ Nm/ $^\circ$.

A. Outcome measures

The non-parametric Friedman's ANOVA revealed that on average the sEMG RMS of the biceps muscle significantly differed among the conditions, see Table III. The Wilcoxon signed rank test revealed that on average, compared to no support (baseline), the muscle activity of the biceps muscle decreased significantly ($p < .01$, $r = -.62$) for the scaled-model (-47.7%), the measured (-21.3%), the hybrid (-39.1%) and the fitted-model (-31.5%) strategy. No significant differences were found between the compensation strategies for the biceps muscles.

On average, the activity in the triceps muscle decreased for the scaled-model (-0.7%), the measured (-3.2%) and the hybrid (-9.6%), but slightly increased for the fitted-model strategy ($+2.2\%$), however these differences were not significant. See Fig. 4.

No statistical significant differences were found for the position-tracking RMS error, the NASA-TLX and the 5-point Likert scale. The NASA-TLX score ranged on average from 31 to 37% among the conditions, meaning that the task load was rated as 'somewhat high' for all conditions. Out of the 12 participants, 4 preferred the scaled-model (33%), 4 preferred

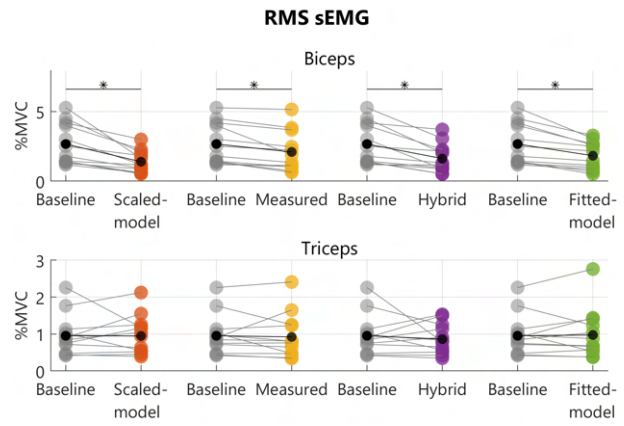


Fig. 4. Scatterplot of RMS sEMG results in the near vertical configuration for biceps (top) and triceps (bottom), normalized to percentage of maximally voluntary contraction (MVC). Based on the data of day 2 (position-tracking task). The black dots represent the group mean.

measured (33%), 3 preferred fitted-model (25%), and 1 the hybrid (8%) compensation strategy.

IV. DISCUSSION

This study is the first exploring different arm support strategies that include weight as well as pJimp compensation. We explored two new combinations of weight and pJimp compensation strategies (hybrid and fitted-model) and compared this with the 'conventional' weight only (scaled-model) and measured strategy similar to Lobo-Prat et al. [8].

All four compensation strategies showed a significant reduction in the anti-gravity biceps muscle activity. No statistically significant differences were found between the compensation strategies. Therefore, it is important to look at the pros and cons of the strategies to decide which strategy is most promising.

A. Comparison of the compensation strategies

The *measured* strategy is expected to be most accurate since it is based on the actual passive joint moments. The disadvantage is that it needs calibration measurements in the plane of movement. This can be a time-consuming and complex process, especially in multi-DOF set-ups. The *fitted-model* has the advantage over the measured strategy that it allows for parameter tuning of either the gravitational (e.g., for thicker clothes) or pJimp (e.g., affected by room temperature) model parameters, potentially reducing the need of re-calibration. Furthermore, the model parameters can be fitted to a set of joint configurations instead of full ROM measurements, reducing the time of the calibration process. The advantage of the *scaled-model* strategy is that only biometric data need to be collected to set the model parameters. However, the scaled-model strategy is missing the pJimp component. Although the pJimp component can easily be overcome by the muscle strength of non-disabled participants, it does seem to play a substantial role (range takes up 60%) in the measured passive joint moments. For the intended target population the pJimp is much higher in

TABLE III
OUTCOME OF THE NON-PARAMETRIC FRIEDMAN'S ANOVA AND GROUP MEAN AND STANDARD DEVIATION

Outcomes	$\chi^2(4)$	p-value	Units	Baseline		Scaled-model		Measured		Hybrid		Fitted-model	
				Mean	SD	Mean	SD	Mean	SD	Mean	SD	Mean	SD
sEMG Biceps RMS	25.93	<.00	%MVC	2.66	1.48	1.39	0.78	2.09	1.44	1.62	1.03	1.82	0.99
sEMG Triceps RMS	5.33	.33	%MVC	0.95	0.53	0.95	0.47	0.92	0.61	0.86	0.4	0.97	0.65
Tracking error RMS	1.60	.81	degrees	2.60	0.62	3.04	1.17	2.85	1.01	2.95	0.78	2.77	0.86
NASA TLX	1.13	.89	%	34.85	16.79	34.32	16.12	36.63	17.62	37.73	17.30	31.17	16.37
5-point Likert-Scale	4.34	.36	1-5	3.58	0.67	3.50	0.80	3.42	0.90	3.08	0.79	3.58	1.00

relation to their muscle strength ($\pm > 50$ times) [3], [28]. The pJimp component introduces a reduction of the passive joint moments in the extension region and an increase in the flexion region. This can be seen with the *hybrid* strategy that shows a slight tilt with respect to the scaled-model. However, this does not seem to explain all the differences between the measured joint moments and the scaled-model. It seems that there is an overestimation of the gravitational model parameters, which holds for both the scaled-model and hybrid strategy. So, a disadvantage of these two strategies is that the model parameters are easily over- or under-estimated using anthropometric tables. Moreover, it is known that the soft tissue composition in the arm of people with for example MD is different to that of non-disabled (e.g., less muscle tissue, more fat and connective tissue) [29], making it even more complex to predict the model parameters with accuracy. The advantage of the hybrid strategy is that only the pJimp needs to be identified instead of full ROM measurements, which can save time in the calibration process. However, when the gravitational component is overestimated, adding an additional pJimp will add an extra support torque in the higher flexion region. Too high anti-gravity support will result in difficulties to move the arms down, as is seen in non-powered arm supports (e.g., by springs) due to imperfect static balancing of the arms [30], [31]. An advantage of powered systems is that the compensation gain can be adjusted in case of model inaccuracies, improving the usability. However, model inaccuracies are sub-optimal and can introduce problems when a high level of accuracy in support level is required for the target population.

Overall, our expectation is that the measured and fitted-model strategies are most promising to test in a target population with severe muscle weakness. Since the scaled-model and hybrid torque-angle profiles seem to overestimate the gravitational component. Moreover, the scaled-model does not take into account the pJimp component, and we have seen that, even in non-disabled, this affects the passive joint moments.

B. Limitations of the study

It is not well known how well these results translate to pathologies with severe muscle weakness and elevated pJimp. We found a way to model and fit the passive joint moments in a combined weight and pJimp model with a linear relation for the pJimp. First of all, more research is needed to determine whether the fitted 1st-order model of the pJimp can be applied in pathologies with elevated pJimp, or

that a higher order or personalized model is required. This study measured the passive joint moments within an elbow ROM of 80% due to safety reasons. Although this covers the ROM for most functional ADL, it is expected that the pJimp is higher at the joint limits, potentially resulting in a higher order fit. Furthermore, potential effects of shoulder positions by for example differences in bi-articular muscles are not taken into account. Moreover, the velocity effects are averaged out and therefore potential damping effects in the pJimp are not taken into account in the compensation strategies. This is in accordance with [32], who also found that the dynamics of the passive human arm depends mostly on the joint angle. Secondly, the non-disabled participants require only little relative muscle effort (%MVC) to perform the position-tracking task. This makes it difficult to find and feel differences between the relatively small changes in the provided support torque. This task is expected to require much larger relative muscle effort (MVC%) in a target population with severe muscle weakness (e.g., 2% elbow flexion moment of healthy population [3], [28]), where the accuracy of the provided support levels become more critical and the compensation efficacy more distinctive. As indication, a 1 Nm difference in support torque can take up 70% of the max elbow flexion moment in MD patients [3].

As mentioned, the parameters used for the hybrid and scaled-model strategies seem to be overestimated. More research in the anthropomorphic characteristics might improve the parameter estimation.

For the practical validity in the clinical application a powered arm support with accurate torque sensing is required, so that the system can both accurately identify the passive joint moments for calibration and provide the accurate support levels. Follow-up studies should identify whether muscle relaxation measurements during calibration is redundant.

V. CONCLUSIONS

All four compensation strategies showed a significant reduction in the anti-gravity muscle activity, but no statistically significant differences were found in the compensation efficacy between the compensation strategies.

It was found that pJimp substantially affects the passive elbow joint moments, even in non-disabled participants. This underlines the necessity of pJimp compensation, which is expected to be even more critical in people who suffer from severe muscle weakness in combination with elevated pJimp.

The profiles of the measured and fitted-model strategies were highly similar, while the scaled-model and hybrid seem

to overestimate the passive joint moments.

Based on the current study, the measured and fitted-model are expected to be the most interesting and promising strategies to test in a follow-up study.

ACKNOWLEDGMENT

We would like to specially thank the voluntary participants who made this study possible. Moreover, BSc Kyriacos Papa and BSc Zhangyue Wei who assisted in conducting the experiments.

REFERENCES

- [1] G. Prange, "Rehabilitation robotics: stimulating restoration of arm function after stroke," Ph.D. dissertation, Roessingh Research & Development, 2009.
- [2] J. Essers, A. Murgia, A. Bergsma, P. Verstegen, and K. Meijer, "An inverse dynamic analysis on the influence of upper limb gravity compensation during reaching," in *2013 IEEE 13th International Conference on Rehabilitation Robotics (ICORR)*, 2013, pp. 1–5.
- [3] D. Ragonesi, S. K. Agrawal, W. Sample, and T. Rahman, "Quantifying anti-gravity torques for the design of a powered exoskeleton," *IEEE Transactions on Neural Systems and Rehabilitation Engineering*, vol. 21, no. 2, pp. 283–288, 2013.
- [4] J. Lobo-Prat, A. Q. Keemink, B. F. Koopman, A. H. Stienen, and P. H. Veltink, "Adaptive gravity and joint stiffness compensation methods for force-controlled arm supports," in *2015 IEEE International Conference on Rehabilitation Robotics (ICORR)*, 2015, pp. 478–483.
- [5] K. L. Boon, A. L. Hof, and W. Wallinga-de Jonge, "The Mechanical Behaviour of the Passive Arm," *Medicine and Sport*, vol. 8, no. Biomechanics III, pp. 243–248, 1973.
- [6] S. Maggioni, A. Melendez-Calderon, E. Van Asseldonk, V. Klamroth-Marganska, L. Lünenburger, R. Riener, and H. Van Der Kooij, "Robot-aided assessment of lower extremity functions: A review," *Journal of NeuroEngineering and Rehabilitation*, vol. 13, no. 1, pp. 1–25, 2016. [Online]. Available: <http://dx.doi.org/10.1186/s12984-016-0180-3>
- [7] M. C. Corrigan and R. A. Foulds, "Evaluation of admittance control as an alternative to passive arm supports to increase upper extremity function for individuals with Duchenne muscular dystrophy," *Muscle and Nerve*, vol. 61, no. 6, pp. 692–701, 2020.
- [8] J. Lobo-Prat, P. N. Kooren, M. M. Janssen, A. Q. Keemink, P. H. Veltink, A. H. Stienen, and B. F. Koopman, "Implementation of EMG-and force-based control interfaces in active elbow supports for men with duchenne muscular dystrophy: a feasibility study," *IEEE Transactions on Neural Systems and Rehabilitation Engineering*, vol. 24, no. 11, pp. 1179–1190, 2016.
- [9] C. Cornu, F. Goubel, and M. Fardeau, "Muscle and joint elastic properties during elbow flexion in Duchenne muscular dystrophy," *The Journal of Physiology*, vol. 533, no. 2, pp. 605–616, 2001. [Online]. Available: <https://onlinelibrary.wiley.com/doi/10.1111/j.1469-7793.2001.0605a.x>
- [10] M. M. Janssen, A. Bergsma, A. C. Geurts, and I. J. De Groot, "Patterns of decline in upper limb function of boys and men with DMD: An international survey," *Journal of Neurology*, vol. 261, no. 7, pp. 1269–1288, 2014.
- [11] M. Lakie, E. G. Walsh, and G. W. Wright, "Control and postural thixotropy of the forearm muscles: Changes caused by cold," *Journal of Neurology Neurosurgery and Psychiatry*, vol. 49, no. 1, pp. 69–76, 1986.
- [12] L.-q. Q. Zhang, H.-s. S. Park, Y. Ren, S. Member, H.-s. S. Park, and Y. Ren, "Shoulder, elbow and wrist stiffness in passive movement and their independent control in voluntary movement post stroke," *2009 IEEE International Conference on Rehabilitation Robotics, ICORR 2009*, pp. 805–811, 2009.
- [13] F. Just, Ö. Özen, S. Tortora, V. Klamroth-Marganska, R. Riener, and G. Rauter, "Human arm weight compensation in rehabilitation robotics: Efficacy of three distinct methods," *Journal of NeuroEngineering and Rehabilitation*, vol. 17, no. 1, pp. 1–17, 2020.
- [14] H. J. Hermens, B. Freriks, C. Disselhorst-Klug, and G. Rau, "Development of recommendations for SEMG sensors and sensor placement procedures," *Journal of Electromyography and Kinesiology*, vol. 10, no. 5, pp. 361–374, 2000.
- [15] D. A. Winter, *Biomechanics and Motor Control of Human Movement: Fourth Edition*, 4th ed. John Wiley & Sons, INC., 2009.
- [16] J. R. Karges, B. E. Mark, S. J. Stikleather, and T. W. Worrell, "Concurrent Validity of Upper- Extremity Volume Estimates :," *Physical therapy*, vol. di, no. 2, pp. 134–145, 2003.
- [17] R. Chandler, C. Clauser, J. McConville, H. M. Reynolds, and J. Yough, "Investigation of Inertial Properties of the Human Body," Aerospace medical research laboratory, Tech. Rep., March 1975.
- [18] C. E. Clauser, J. T. McConville, and J. W. Young, "Weight, volume, and center of mass of segments of the human body," Aerospace medical research laboratory, Tech. Rep., August 1969.
- [19] W. Dempster, "Space requirements of the seated operator," Wright Patterson Air Force Base, Tech. Rep., 1955.
- [20] W. F. Rampeltshammer, A. Q. Keemink, and H. Van Der Kooij, "An Improved Force Controller with Low and Passive Apparent Impedance for Series Elastic Actuators," *IEEE/ASME Transactions on Mechatronics*, vol. 25, no. 3, pp. 1220–1230, 2020.
- [21] M. M. Janssen, J. Horstik, P. Klap, and I. J. de Groot, "Feasibility and effectiveness of a novel dynamic arm support in persons with spinal muscular atrophy and duchenne muscular dystrophy," *Journal of NeuroEngineering and Rehabilitation*, vol. 18, no. 1, pp. 1–13, 2021. [Online]. Available: <https://doi.org/10.1186/s12984-021-00868-6>
- [22] P. N. Kooren, A. G. Dunning, M. M. Janssen, J. Lobo-Prat, B. F. Koopman, M. I. Paalman, I. J. De Groot, and J. L. Herder, "Design and pilot validation of A-gear: A novel wearable dynamic arm support," *Journal of NeuroEngineering and Rehabilitation*, vol. 12, no. 1, pp. 1–12, 2015. [Online]. Available: <http://dx.doi.org/10.1186/s12984-015-0072-y>
- [23] J. Essers, A. Murgia, A. A. Peters, M. M. Janssen, and K. Meijer, "Recommendations for studies on dynamic arm support devices in people with neuromuscular disorders: a scoping review with expert-based discussion," *Disability and Rehabilitation: Assistive Technology*, vol. 0, no. 0, pp. 1–14, 2020. [Online]. Available: <https://doi.org/10.1080/17483107.2020.1806937>
- [24] P. So, "NASA Task Load index nasa tlx : ios app," 2020. [Online]. Available: <https://humansystems.arc.nasa.gov/groups/tlx/tlxapp.php>
- [25] Y. Benjamini and D. Yekutieli, "The control of the false discovery rate in multiple testing under dependency," *Annals of statistics*, pp. 1165–1188, 2001.
- [26] M. E. Glickman, S. R. Rao, and M. R. Schultz, "False discovery rate control is a recommended alternative to Bonferroni-type adjustments in health studies," *Journal of Clinical Epidemiology*, vol. 67, no. 8, pp. 850–857, 2014. [Online]. Available: <http://dx.doi.org/10.1016/j.jclinepi.2014.03.012>
- [27] A. Field, *Discovering statistics using IBM SPSS statistics*, 4th ed. sage, March 2013.
- [28] L. J. Hébert, D. B. Maltais, C. Lepage, J. Saulnier, and M. Crête, "Hand-Held Dynamometry Isometric Torque Reference Values for Children and Adolescents," *Pediatric Physical Therapy*, vol. 27, no. 4, pp. 414–423, 2015.
- [29] V. Ricotti, M. R. Evans, C. D. Sinclair, J. W. Butler, D. A. Ridout, J. Y. Hogrel, A. Emira, J. M. Morrow, M. M. Reilly, M. G. Hanna, R. L. Janiczek, P. M. Matthews, T. A. Yousry, F. Muntoni, and J. S. Thornton, "Upper limb evaluation in duchenne muscular dystrophy: Fat-water quantification by MRI, muscle force and function define endpoints for clinical trials," *PLoS ONE*, vol. 11, no. 9, pp. 1–15, 2016.
- [30] V. Longatelli, A. Antonietti, E. Biffi, E. Diella, M. G. D'Angelo, M. Rossini, F. Molteni, M. Bocciolone, A. Pedrocchi, and M. Gandolla, "User-centred assistive System for arm Functions in neUromuscular subjects (USEFUL): a randomized controlled study," *Journal of NeuroEngineering and Rehabilitation*, vol. 18, no. 1, pp. 1–17, 2021. [Online]. Available: <https://doi.org/10.1186/s12984-020-00794-z>
- [31] T. Estilow, A. M. Glanzman, K. Powers, A. Moll, J. Flickinger, L. Medne, G. Tennekoon, and S. W. Yum, "Use of the wilmington robotic exoskeleton to improve upper extremity function in patients with duchenne muscular dystrophy," *American Journal of Occupational Therapy*, vol. 72, no. 2, pp. 1–5, 2018.
- [32] M. Guidali, U. Keller, V. Klamroth-Marganska, T. Nef, and R. Riener, "Estimating the patient's contribution during robot-assisted therapy," *Journal of Rehabilitation Research and Development*, vol. 50, no. 3, pp. 379–394, 2013.